Rare Metal Materials and Engineering
Volume 49, Issue 8, August 2020
Available online at www.rmme.ac.cn

Science Press

Cite this article as: Rare Metal Materials and Engineering, 2020, 49(8): 2557-2566.

ARTICLE

First-principles Investigation on Formation Energy, Elasticity and Interfacial Properties of Refining Phase $Al_3(Zr, Sc)$ in Al Alloys

Li Chunmei, Jiang Xianquan, Cheng Nanpu, Tang Jianfeng, Chen Zhiqian

Southwest University, Chongqing 400715, China

Abstract: Microalloying is an important means for strengthening aluminum alloys. Sc has attracted much attention as a refiner for aluminum alloys. The addition of Zr and Sc in aluminum matrix can achieve better grain refinement, due to the formation of $Al_3(Zr, Sc)$ refining phase in the aluminum matrix. Based on the first-principles density functional theory, the energy and elastic properties of $Al_3(Zr, Sc)$ formed under different ratios of Sc/Zr were studied. Besides, the interfacial properties of $Al_3(Zr, Sc)$ and Al matrix were also investigated. The results show that when Sc/Zr ratio is not higher than 1/3, the refining phase prefers to precipitate as $Al_3(Zr, Sc)$ based on its larger absolute value of formation enthalpy. And the addition of Sc element is also beneficial to the formation of the interface and the improvement of the interface bonding strength with better wetting effect, but the excessive increase of Sc/Zr ratio to higher than 1/3 shows no positive effect on the improvement of the interface performance. Additionally, the co-addition of Zr and Sc can improve the elastic properties and weaken the anisotropy of Al_3Sc while greatly reduce the cost of the alloy.

Key words: refining phase; formation energy; elastic property; interfacial property; $Al_3(Zr, Sc)$

Al-Zn-Mg-Cu alloy has excellent performance, high specific strength, high specific stiffness, good corrosion resistance, high toughness, good elasticity, excellent impact resistance, high electrical conductivity and high thermal conductivity[1-3]. So it is widely used as structural materials in aerospace and various types of hulls. In order to improve its overall performance, microalloying has become one of the main ways. By adding trace elements such as Ti, Zr or Sc, different micro-alloy phases form, thereby achieving fine-grain strengthening, together with sub-structure strengthening and dispersion strengthening effects[4-6]. Al_3Zr, as a refining phase of Al alloy, has the same $L1_2$, $D0_{23}$ or $D0_{22}$ type structure as Al_3Sc. The crystal constants of the Al matrix, Al_3Zr and Al_3Sc are very close, so Al_3Zr and Al_3Sc can precipitate in a coherent interface structure with Al matrix[7-9].

The experimental study indicates that Al_3Zr is more stable than Al_3Sc, and $Al_3(Zr, Sc)$ microalloying phases are more likely to precipitate and stabilize than Al_3Zr and Al_3Sc. The effect of $Al_3(Zr, Sc)$ microalloying phase pinning dislocation is enhanced and dispersed[10-13]. In terms of performance improvement, when Sc is added alone, the tensile strength and elongation of the alloy are significantly higher than adding Zr alone, but the effect of suppressing recrystallization is weaker when Sc is added alone than when Zr is added alone[14-16]. Simultaneous addition of Sc and Zr elements in the Al alloy can significantly refine the as-cast grains of the alloy and extremely improve the mechanical properties of the alloy[17]. The main reason is that $Al_3(Zr, Sc)$ heterogeneous nucleation can refine the as-cast grains of the alloy, and produce pinning effect, which effectively hinders grain boundary migration and dislocation sliding, and inhibits alloy recrystallization, then achieving fine grain strengthening, substructure strengthening and dispersion strengthening[9,15,18-21]. Therefore, the formation of the $Al_3(Zr, Sc)$ microalloying phase can not only improve

Received date: August 29, 2019
Foundation item: National Natural Science Foundation of China (51601153); Chongqing Research Program of Basic Research and Frontier Technology (cstc2017jcyjAX0195); Fundamental Research Funds for the Central Universities (XDJK2018C004)
Corresponding author: Li Chunmei, Ph. D., Associate Professor, School of Materials and Energy, Southwest University, Chongqing 400715, P. R. China, Tel: 0086-23-68254376, E-mail: lcm1998@swu.edu.cn

the overall performance of the aluminum matrix, but also effectively reduce the cost[11,14,17,22].

However, there is no systematic research report on the ratio of Zr and Sc elements. At the same time, it is difficult to analyze the precipitation energy and self-property of Al_3(Zr, Sc) phase. Therefore, this work used the first-principles method to systematically study the Al_3(Zr, Sc) phase formed by the microalloying elements Sc and Zr under different ratios. Based on the calculation of energy, the difficulty and the pinning effect of Al_3(Zr, Sc) phase under different Sc/Zr ratios were judged. The elasticity and interfacial properties of Al_3(Zr, Sc) phase with different Sc/Zr ratios in Al matrix were also calculated to analyze the strengthening characteristics of each phase.

1 Calculation

Al is a face-centered cubic (fcc) structure and its space group is FM-3M. The structure of Al_3Zr and Al_3Sc is $D0_{23}$ type tetragonal structure[13,22], and the lattice constant is shown in Table 1. Since the Al_3Zr and Al_3Sc phases are coherent with Al matrix, we chose Al_3Zr crystal as the original unit cell for doping. In order to deeply analyze the energy and elastic properties of Al_3(Zr, Sc) formed under different Sc/Zr ratios, a 2×2×1 super-cell based on the unit cell of Al_3Zr was constructed for doping. Then, according to the Sc/Zr ratio, atomic substitution was performed to construct Al_3(Zr, Sc) with different ratios. With the same Sc/Zr ratio, we consider different doping sites for permutation based on symmetry, and perform system calculations to find the most stable doping phase. In order to reduce the amount of calculation, the symmetry is re-searched and added to the super-cell after Sc replacement, and the calculation unit of Al_3(Zr, Sc) with different Sc/Zr ratios was obtained. Fig.1 shows the most stable doped structures with different Sc/Zr ratios. During the theoretical calculation process, in order to obtain a stable structural model, geometric optimization of each model was performed. All calculations of energy, elastic properties and electronic properties were performed after all atoms were fully relaxed.

Experimental results show that Al_3(Zr, Sc)(001)/Al(001) interface mode is one of the most common interface formation orientation of Al_3(Zr, Sc) particles precipitated in the Al matrix[22]. Here, to focus on the influence of Sc/Zr ratio on the interfacial binding energy, different interfaces with various terminations of Al_3(Zr, Sc) phase were built perpendicular to $[001]_{Al}$ crystal orientation. According to our former investigation on the interfacial properties of Al_3TM (*TM*=Ti, Zr, Hf, Sc) in Al matrix[22], the surfaces of Al_3(Zr, Sc) including Zr or Sc atoms that conjunct directly with Al matrix in central-site stacking mode should be the most stable. This model maintains the periodic structure of Al matrix and is coherent well with the matrix. To investigate different conjunction modes of Al_3(Zr, Sc) phase with Al matrix, various terminations of Al_3(Zr, Sc) phase were considered. So the Al_3(Zr, Sc) phases with different Sc/Zr ratios were cut from different planes to form surfaces with Sc or Zr atoms located at the surface. All the non-equivalent terminations of Al_3(Zr, Sc) phases are shown in Fig.1c as surfaces 1~4.

Table 1 Lattice parameters of calculated Al_3(Zr, Sc) models with different Sc/Zr ratios

Phase	Crystal system	Space group	*a*/nm	*b*/nm	*c*/nm
Al	Cubic	FM-3M	0.4053	0.4053	0.4053
			0.4049[32]	0.4049[32]	0.4049[32]
			0.4044[33]	0.4044[33]	0.4044[33]
Al_3Zr	Tetragonal	I4/MMM	0.4023	0.4023	1.7353
			0.4008[34]	0.4008[34]	1.736[35]
			0.402[35]	0.402[35]	1.732[36]
			0.4013[36]	0.4013[36]	
$Al_{24}Zr_7Sc$	Tetragonal	P4/MMM	0.5690	0.5690	1.7324
$Al_{12}Zr_3Sc$	Tetragonal	P4/MMM	0.5699	0.5699	1.7295
Al_6ZrSc	Monoclinic	P2	0.8107	0.8115	1.7437
$Al_{12}ZrSc_3$	Tetragonal	P4MM	0.5718	0.5718	1.7273
Al_3Sc	Tetragonal	I4/MMM	0.4047	0.4047	1.7277

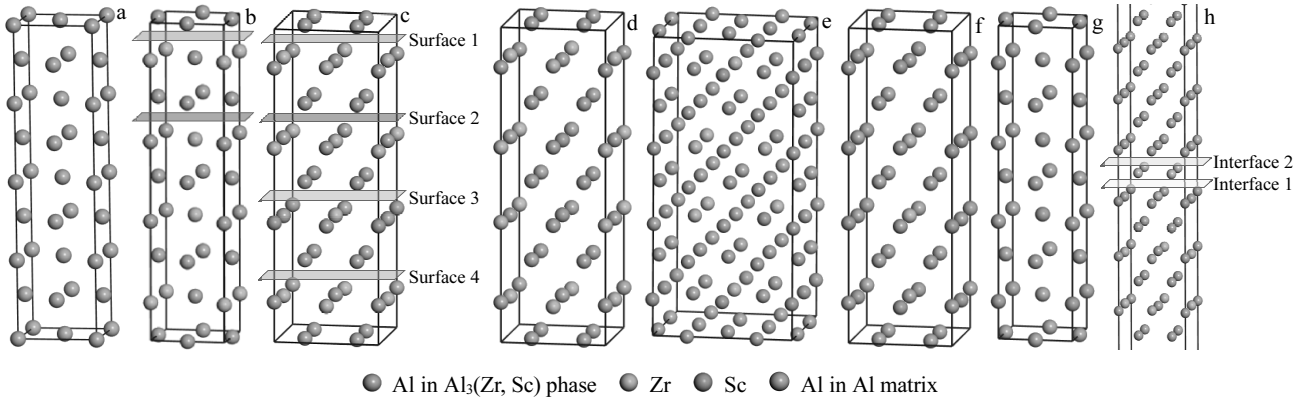

Fig.1 Crystal and interface structures of Al matrix and Al_3(Zr, Sc) phases with different Sc/Zr ratios: (a) Al matrix in 1×1×4 supercell, (b) Al_3Zr with two different termination planes, (c) $Al_{24}Zr_7Sc$ with four different termination planes, (d) $Al_{12}Zr_3Sc$, (e) Al_6ZrSc, (f) $Al_{12}ZrSc_3$, (g) Al_3Sc, and (h) interface model formed of $Al_{24}Zr_7Sc$ in surface 3 with Al matrix including two different interface separation modes

For Al_3Sc and Al_3Zr phases, surfaces 3 and 4 are equivalent to surfaces 1 and 2, so only two types of terminations were considered. To build interface between Al_3(Zr, Sc) phase and Al matrix, the layer numbers of Al_3(Zr, Sc) phase and Al matrix were both set as 9 layers based on convergence test. During calculation, the vacuum was kept as 1.5 nm and three layer of atoms were constrained at both ends to be simulated as the substrate. The interfaces are separated from two different sites, as shown in Fig.1h, as interfaces 1 and 2 to judge the binding properties.

All calculations were carried out by the pseudo-potential plane-wave method[23] and the Cambridge Serial Total Energy Package Program[24]. The electronic exchange-correlation energy was considered using the generalized gradient approximation of Perdew-Burke-Ernzerh (GGA-PBE)[25,26]. Energy cutoff and *k*-points[27] were carefully determined according to the convergence of results. A plane-wave basis set was applied with an energy cutoff of 330 eV. All calculations were performed on a Monkhorst-pack *k*-point mesh with spacing of 0.04 nm^{-1} for the Brillouin zone of the bulk structures.

The second-order elastic constants were calculated by linear fitting the stress-strain curves[28]. Several different types of Lagrangian strain were applied on crystals and Cauchy stress for each strain was calculated after optimizing the internal degrees of freedom. The elastic constants can be obtained by calculating the total energy as a function of the strains[29]. Hook's law is applicable for small strains on solids[30]. The elastic energy ΔE can be expressed as the quadratic function (Eq.(1)) of the strains[31]:

$$\Delta E = V\sum_{i,j=1}^{6}\frac{1}{2}C_{i,j}e_ie_j \quad (1)$$

where V represents the total volume of unit cell, C_{ij} is the elastic constant. Subscripts i and j denote the components of the strain matrix, as shown in Eq.(2):

$$\varepsilon' = \begin{pmatrix} e_1 & e_6 & e_5 \\ e_6 & e_2 & e_4 \\ e_5 & e_4 & e_3 \end{pmatrix} \quad (2)$$

2 Results and Discussion

2.1 Binding energy and formation enthalpy

Binding energy is defined as the energy that is released when two or more free states of atoms are joined together. The binding energy (E_b) can be obtained by Eq.(3):

$$E_b^{A_{n_1}B_{n_2}} = -\left[E_t^{A_{n_1}B_{n_2}} - n_1E_a^A - n_2E_a^B\right]/(n_1+n_2) \quad (3)$$

In the formula, $E_t^{A_{n_1}B_{n_2}}$ represents the total energy of the Al_3(Zr,Sc) calculation unit, and E_a^A and E_a^B are the enthalpies of the individual free atoms A and B, respectively. n_1, n_2 denote the number of atoms in the calculation unit of elements A and B, respectively. The calculated single atomic enthalpies of Al, Zr, and Sc are −52.81, −1273.94, and −1272.80 eV, respectively. The binding energies of Al_3(Zr, Sc) with different Sc/Zr ratios are shown in Table 2. The binding energy reflects the strength of the atomic bonding in the crystal, reflecting the stability of the compound. It can be seen from the calculation results that the absolute value of Al_3Zr's binding energy is the largest, which means that the energy released during the formation of the compound is the largest, so this microalloying phase is most stable, as shown in Fig.2. As the Sc/Zr ratio is lower than 1/3, the binding energy data of them are approximate, and the absolute values are all above 480 kJ/mol, indicating that the Al_3(Zr, Sc) phases with high stability are formed when the Sc/Zr ratio is lower than 1/3. When the

Table 2 Formation enthalpy (ΔH) and binding energy (E_b) of the calculated Al_3(Zr, Sc) phases with different Sc/Zr ratios

Phase	E_b/eV	E_b/kJ·mol^{-1}	$\triangle H$/eV	$\triangle H$/kJ·mol^{-1}
Al_3Zr	−5.01	−499.02	−0.51 −0.48[8]	−50.83 −49.11[33, 37]
$Al_{24}Zr_7Sc$	−4.93	−491.12	−0.51	−51.27
$Al_{12}Zr_3Sc$	−4.84	−482.00	−0.51	−50.47
Al_6ZrSc	−4.65	−462.86	−0.48	−47.97
$Al_{12}ZrSc_3$	−4.46	−444.49	−0.46	−46.26
Al_3Sc	−4.27	−425.41	−0.44 −0.47[38] −0.46[39]	−43.83

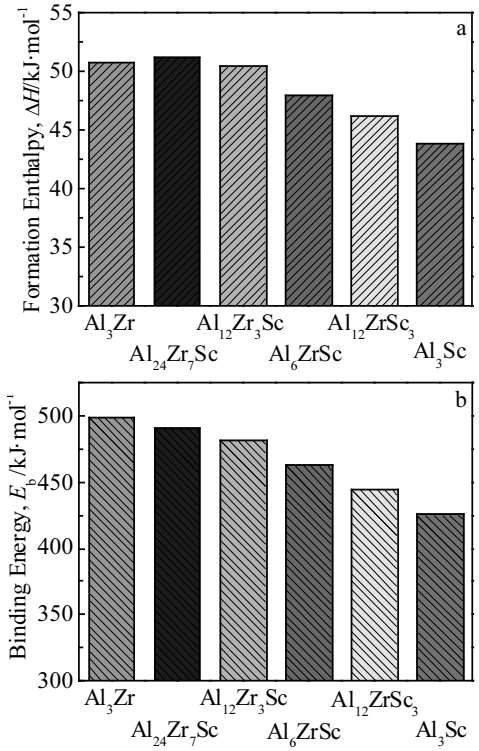

Fig.2 Formation enthalpy (ΔH) and binding energy (E_b) of the calculated Al_3(Zr, Sc) phases with different Sc/Zr ratios

Sc/Zr ratio is higher than 1/3, the absolute value of the binding energy is significantly reduced, and the stability of the formed Al_3(Zr, Sc) phase is not high enough. The addition of too much Sc affects the stability of Al_3(Zr, Sc).

The greater the binding energy, the less easily the compound will decompose, so the reaction generally has a high melting point. From the perspective of the refinement phase, the larger the binding energy, the earlier the nucleation will occur during the casting process, and the refining phase which preferentially nucleates can effectively control the size of the aluminum alloy crystal grains. In addition, the large bonding energy ensures that the refining phase is not easily decomposed during the heat treatment process, thereby further performing pinning action during the heat treatment process, and hindering dislocation slip and grain recrystallization. From these two aspects, for the refinement phase, the large bond energy is advantageous for the improvement of the alloy properties. From the data in the Table, we can see that the absolute value of the binding energy of Al_3Sc is the smallest, which explains why Al_3Zr is more stable than Al_3Sc in the experiment, and why the inhibition recrystallization effect is weaker when adding Sc alone compared to adding Zr alone.

The formation enthalpy (ΔH) can be obtained by Eq.(4):

$$\Delta H_{A_{n_1}B_{n_2}} = \left[E_{\mathrm{t}}^{A_{n_1}B_{n_2}} - n_1 E_{\mathrm{S}}^{A} - n_2 E_{\mathrm{S}}^{B} \right] / (n_1 + n_2) \quad (4)$$

where $E_{\mathrm{t}}^{A_{n_1}B_{n_2}}$ represents the total energy of the Al_3(Zr,Sc) calculation unit; E_{S}^{A} and E_{S}^{B} denote the single atomic energy in the A and B elemental mass, respectively; n_1 and n_2 are the number of atoms in the calculation unit of elements A and B, respectively. In order to ensure the uniformity of the calculated values, the potential fields of the alloy phases and the bulk pure metals were set as the same with the same precision. The single atomic enthalpy values of bulk Al, Zr, and Sc are −56.43, −1281.05, and −1277.24 eV, respectively. The formation of microalloying phase can be obtained by the above formula, and the formation enthalpies of Al_3(Zr, Sc) formed under different ratios are shown in Table 2. The formation enthalpy indicates the energy absorbed or released by the compound during its formation, and its value determines the ease of the formation of compound. The formation enthalpy is a negative value, and the larger the absolute value, the easier the corresponding compound can be formed. It can be seen from the data in Table 2 that the absolute value of the formation enthalpy of Al_3(Zr, Sc) is greater than the absolute value of the binding energy of Al_3Zr and Al_3Sc with Sc/Zr ratio of 1/7. This indicates that the simultaneous addition of Sc and Zr induces a larger nucleation driving force, which is beneficial to the nucleation of Al_3(Zr, Sc) and the dispersion distribution of the fine crystal phase. When the Sc/Zr ratio is less than 1/3, the difference in the formation energy is not large, and the absolute value is above 50 kJ/mol, indicating that these Al_3(Zr, Sc) phases are easier to form when the Sc/Zr ratio is less than 1/3. When the Sc/Zr ratio is higher than 1/3, the absolute value of the formation enthalpy is remarkably lowered, and the driving force to form these high Sc-concentration Al_3(Zr, Sc) phases becomes small. So in experiments, since the formation of Al_3Zr, $Al_{24}Zr_7Sc$ and $Al_{12}Zr_3Sc$ phases is easier, they will nucleate first, then excess Sc will form Al_6ScZr, $Al_{12}ZrSc_3$ and Al_3Sc phases with higher Sc/Zr ratio. This also indicates why the Al_3(Zr, Sc) microalloying phase is more likely to precipitate than Al_3Zr and Al_3Sc in experiments[10,13,40]. In terms of the difficulty of nucleation, they are more inclined to nucleate and attach on the original precipitation phase. So excessive Sc doping will affect the formation of Al_3(Zr, Sc) in reverse. Therefore, from the result of the formation enthalpy of Al_3(Zr, Sc), it can be inferred that when the Sc/Zr ratio is less than 1/3, not only the cost can be effectively reduced, but also the nucleation of Al_3(Zr, Sc) is favored.

2.2 Elastic properties

Elastic modulus is an important performance index of materials. From a macro perspective, elastic modulus is a measure of the ability of an object to resist elastic deformation. From a microscopic perspective, it reflects the strong or weak bonding between atoms, ions or molecules. In this work, using the Voigt-Reuss-Hill approximation, based on the elastic stiffness matrix (Table 3), the elastic properties, bulk modulus, shear modulus, and Young's modulus of Al_3(Zr, Sc) phases with different ratios are calculated. The amount and anisotropy index are shown in Table 4.

The bulk modulus B can reflect the macroscopic property of a material. The greater the B value, the stronger the ability to resist deformation. It can be deduced from the calculation results in Table 4 that Al_3Zr has the strongest stiffness. As the Sc content increases, the stiffness becomes weaker. When the Sc/Zr ratio is lower than 1/3, the stiffness of Al_3Zr, $Al_{24}Zr_7Sc$ and $Al_{12}Zr_3Sc$ is high overall, both higher than 95 GPa. When the Sc/Zr ratio is higher than 1/3, the stiffness of Al_6ZrSc, $Al_{12}ZrSc_3$ and Al_3Sc is generally low, about 80 GPa.

Shear modulus G is used to characterize the material's ability to resist shear strain. The greater the value, the tougher the material. Comparing the data in Table 4, Al_3(Zr, Sc) with Sc/Zr ratio of 1/3 has the strongest resistance to shear strain except the pure Al_3Zr phase. The changing trend of shear

Table 3 Elastic constants C_{ij} of Al_3(Zr,Sc) phases with different Sc/Zr ratios (GPa)

Phase	C_{11}	C_{12}	C_{13}	C_{33}	C_{44}	C_{66}
Al_3Zr	203.11	63.15	43.21	201.54	83.61	103.27
	201.5[8]	68.6[8]	44.1[8]	199.8[8]	81.6[8]	102.9[8]
	201.3[41]	67[41]	40.6[41]	196.7[41]	80.8[41]	102.6[41]
$Al_{24}Zr_7Sc$	234.63	27.68	41.88	201.90	76.95	64.65
$Al_{12}Zr_3Sc$	188.49	71.28	37.08	201.59	75.62	97.07
Al_6ZrSc	164.76	31.54	36.70	163.25	86.62	69.38
$Al_{12}ZrSc_3$	152.16	49.52	37.19	147.88	66.21	89.52
Al_3Sc	170.07	54.82	28.94	173.36	68.63	99.85

Table 4 Calculated bulk modulus *B*, shear modulus *G*, Young's modulus *E*, *B*/*G*, Poisson's ratio, anisotropy coefficient A^U for Al_3(Zr, Sc) phases with different Sc/Zr ratios

Phases	Al_3Zr	$Al_{24}Zr_7Sc$	$Al_{12}Zr_3Sc$	Al_6ZrSc	$Al_{12}ZrSc_3$	Al_3Sc
B_V/GPa	100.8	99.3	97.1	82.2	77.9	82.1
B_R/GPa	100.6	99.2	96.9	82.0	77.7	81.9
B/GPa	100.7 106.6[8] 102.1[41]	99.3	97.0	82.1	77.8	82.0
G_V/GPa	84.6	81.0	82.6	70.4	66.2	74.1
G_R/GPa	83.3	79.1	81.2	69.1	63.9	71.7
G/GPa	84.0 85.7[8] 82.3[41]	80.1	81.9	69.8	65.1	72.9
B/*G*	1.20 1.24[8]	1.24	1.19	1.18	1.20	1.12
E/GPa	197.1 202.8[8] 194.5[41]	189.3	191.7	163.1	152.7	168.7
v	0.17 0.18[8]	0.18	0.17	0.17	0.17	0.16
A^U	0.08 0.07[8] 0.08[41]	0.12	0.09	0.10	0.18	0.17

strain data with increasing the Sc/Zr ratio is similar to that of the bulk modulus value. When the Sc/Zr ratio is lower than 1/3, the *G* values of Al_3Zr, $Al_{24}Zr_7Sc$ and $Al_{12}Zr_3Sc$ are totally higher, all higher than 80 GPa. When the Sc/Zr ratio is higher than 1/3, the *G* values of Al_6ZrSc and $Al_{12}ZrSc_3$ are generally low, less than 70 GPa except for the pure Al_3Sc phase.

The Young's modulus *E* is obtained by Eq.(5)

$$E=9BG/(3B+G) \quad (5)$$

Young's modulus *E* can measure the difficulty of elastic deformation of a material, and the larger the value, the greater the stress required for the material to deform elastically. Comparing the data in the Table, when the Sc/Zr ratio equals 1/3, the stress required for $Al_{12}Zr_3Sc$ phase to strain is the largest, so its ability to resist elastic deformation of the material is the strongest. The Young's modulus *E* data are also divided into two parts by the Sc/Zr ratio of 1/3. When the Sc/Zr ratio is less than 1/3, the elastic strengths of Al_3Zr, $Al_{24}Zr_7Sc$ and $Al_{12}Zr_3Sc$ are all high, both higher than 190 GPa. When the Sc/Zr ratio is higher than 1/3, the elastic strengths of Al_6ZrSc, $Al_{12}ZrSc_3$ and Al_3Sc are lower in the whole, all lower than 170 GPa.

As a result, based on the three main parameters of the elastic properties including the bulk modulus *B*, the shear modulus *G* and the Young's modulus *E*, when the aluminum alloy microalloying elements Sc and Zr are simultaneously added, the Sc/Zr ratio should not be higher than 1:3. Otherwise, the elastic properties of the Al_3(Zr, Sc) phases will drop significantly, which will have a negative influence on the strengthening effect of the Al alloy.

According to the Pugh criterion, the toughness and brittleness of materials are related to *B*/*G*[13]. When the *B*/*G* ratio is greater than 1.75, the material behaves as toughness and vice versa. The data in Table 4 shows that all the *B*/*G* values corresponding to different ratios of Al_3(Zr, Sc) are less than 1.75, so Al_3(Zr, Sc) phase should be a brittle material, which is also a universal characteristic of the strengthening phase of the aluminum alloy. However, the overall data show that the toughness of the Al_3(Zr, Sc) phase obtained by adding both Sc and Zr is better than that of the Al_3Sc phase formed by simply adding Sc. Among them, $Al_{24}Zr_7Sc$ phase with Sc/Zr ratio of 1/7 has the largest *B*/*G* value, so this phase has the relatively best ductility.

The Poisson's ratio (*v*) of the material can be used to assess the material's ability to resist shear deformation, and the magnitude of *v* is also related to the brittleness and toughness of the material. The greater the Poisson's ratio (*v*) value, the better the plasticity of the material. Here, the Poisson's ratio is obtained by Eq.(6).

$$v=\frac{1}{2}\left(\frac{B-(2/3)G}{B+(1/3)G}\right) \quad (6)$$

From the Poisson's ratio values shown in Table 4, it can be seen that when Sc/Zr ratio equals 1/7, the corresponding $Al_{24}Zr_7Sc$ phase has the largest Poisson's ratio, and its plasticity should be the best. Similar to the law of *B*/*G* values, the shear resistance of the Al_3(Zr, Sc) phases obtained by adding Sc and Zr simultaneously is better than that of the Al_3Sc phase formed by simply adding Sc.

Whether the strengthening phase in the aluminum alloy easily induces microcracks during the deformation process of the aluminum alloy is related to the anisotropy of the strengthening phase. If the elastic anisotropy of the strengthening phase is severe, it is easy to induce the germination of microcracks in the matrix during the deformation process. Using Eq.(7) proposed by Ranganathan and Ostoja-Starzewski, we calculated the anisotropy factor A^U of different Al_3(Zr, Sc) phases.

$$A^U=5\frac{G_V}{G_R}+\frac{B_V}{B_R}-6\geqslant 0 \quad (7)$$

If the crystal is isotropic, the anisotropy factor A^U should be zero, that is, the closer the anisotropic factor A^U value to zero, the weaker the anisotropy. The data of A^U in Table 4 show that the value of Al_3Zr is the smallest and the value of Al_3Sc is the largest. The calculation results show that the simultaneous addition of Sc and Zr can effectively improve the anisotropy of the Al_3Sc phase. When the Sc/Zr ratio is less than 1:1, the anisotropy of the Al_3(Zr, Sc) phase is weak overall. When Sc/Zr equals 1/3, the A^U value is the smallest, the anisotropy is the weakest, and the microcrack is the least likely to appear.

In order to visually describe the elastic anisotropy of the Al_3(Zr, Sc) phase under different Sc/Zr ratios, the three-dimensional surface profile and elastic modulus of Young's

modulus of $Al_3(Zr, Sc)$ under different ratios were drawn. They are projected on the *XX*, *XZ* and *YZ* planes, as shown in Fig.3. The Young's modulus changes of the tetragonal system with the orientation of the crystal can be obtained by Eq.(8)

$$E_T = 1/[(l_1^4 + l_2^4)S_{11} + l_3^4 S_{33} + l_1^2 l_2^2 (2S_{12} + S_{66}) + l_3^2 (1 - l_3^2)(2S_{13} + S_{44}) + 2l_1 l_2 (l_1^2 - l_2^2) S_{16}] \quad (8)$$

where S_{ij} represents the elastic smoothness coefficient, l_1, l_2 and l_3 denote the direction cosine of the crystal orientation with respect to the *X*, *Y*, and *Z* axes, respectively.

2.3 Interfacial property

The Griffith rupture work (W_{ad}) [22] is defined as the energy required for per unit area to reversibly separate a bulk material into two semi-infinite bulks with two free surfaces. It is sometimes called the "ideal work of separation." In this study, W_{ad} is calculated according to Eq.(9).

$$W_{ab}=[E_{Al_3(Zr,Sc)}+E_{Al}-E_{Al_3(Zr,Sc)/Al}]/A \quad (9)$$

where $E_{Al_3(Zr,Sc)/Al}$ represents the total interfacial energy embedded in vacuum; $E_{Al_3(Zr,Sc)}$ and E_{Al} denote the total energies of $Al_3(Zr, Sc)$ and α-Al with free surfaces, respectively; *A* is the area of the interface. All systems are calculated under exactly the same conditions (*k*-points, cutoff energy, etc). They are all subjected to the lattice parameters of Al matrix because all the phase is precipitated in Al matrix and coherent with Al matrix. Perpendicularly to the interface, all the atoms are fully relaxed during the calculation. The Griffith rupture work calculated in this manner gives direct information regarding the strength and bonding of the interface and is taken as a measure for the mechanical stability and chemical bonding strength at the interface.

Fig.4 plots the Griffith rupture work (W_{ad}) of the interfaces both in interface 1 and 2 modes shown in Fig.1. Several conclusions can be drawn from the data. Firstly, the Griffith rupture work (W_{ad}) of all the interface in interface 1 mode (Fig.4a) shows higher values than those in interface 2 modes (Fig.4b), which means that the direct combination of Al with $Al_3(Zr, Sc)$ is difficult to be broken up during deformation. Secondly, it also shows that the W_{ad} values of Al-$Al_3(Zr, Sc)$ interfaces with the simultaneous addition of Sc and Zr are overall higher than those of Al-Al_3Sc model and Al-Al_3Zr model, both for interface 1 and 2 modes, which means that the addition of Zr and Sc elements together is beneficial to the interfacial binding strength. But under the condition that the Sc/Zr ratio reaches 1/3, the further increasing of Sc/Zr ratio is unfavorable to the W_{ad} values of Al-$Al_3(Zr, Sc)$ interfaces. Thirdly, Al-$Al_3(Zr, Sc)$ interfaces with Sc/Zr ratio less than or equal to 1/3 get larger W_{ad} values in a whole, especially in interface 1 modes. This is easy to understand that interface 1

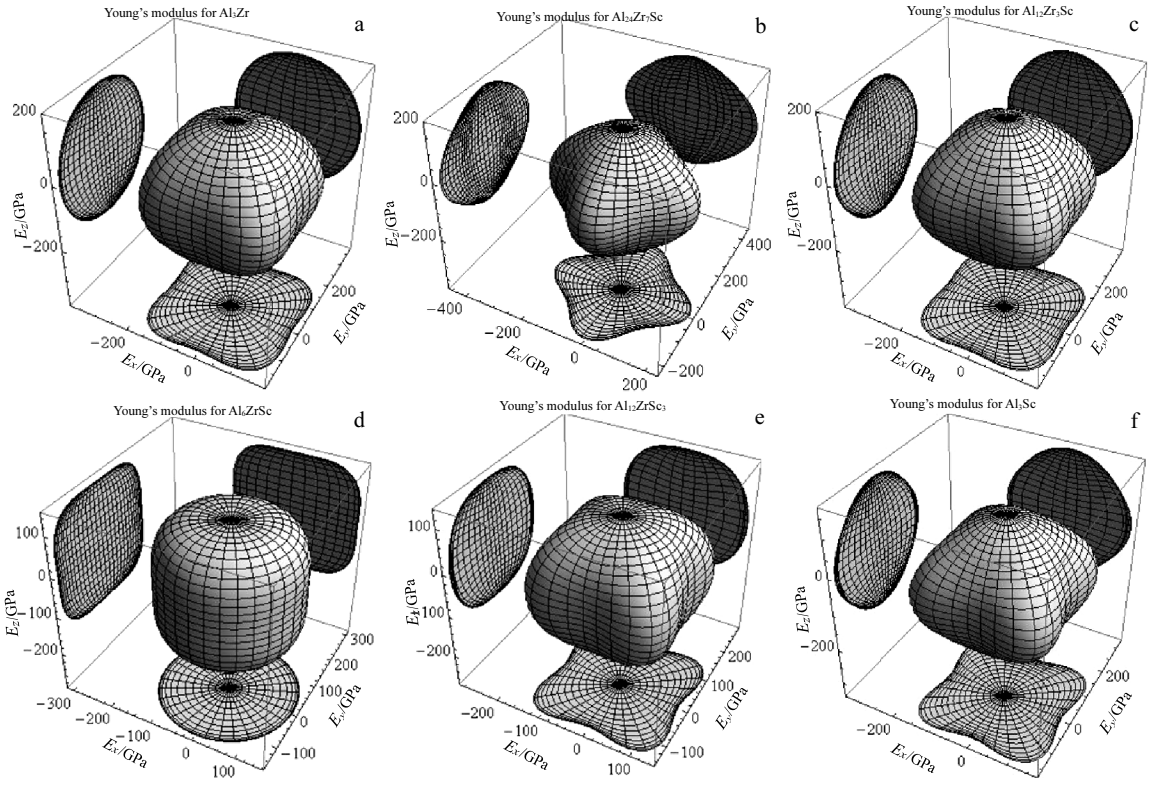

Fig.3 Directional dependences of bulk and Young's moduli for $Al_3(Zr, Sc)$ phases with different Sc/Zr ratios (with projections of the directional dependent moduli on different planes): (a) Al_3Zr, (b) $Al_{24}Zr_7Sc$, (c) $Al_{12}Zr_3Sc$, (d) Al_6ZrSc, (e) $Al_{12}ZrSc_3$, and (f) Al_3Sc

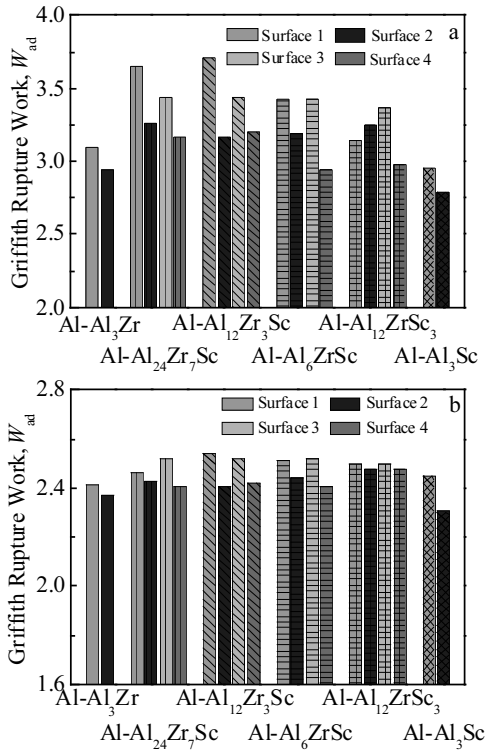

Fig.4 Griffith rupture work (W_{ad}) of different interfaces between Al_3(Zr, Sc) with different Sc/Zr ratios and Al matrix: (a) interface 1 mode and (b) interface 2 mode

modes act as the interior binding mode in Al_3(Zr, Sc) phase. So W_{ad} in interface 1 modes is partly dominated by the formation energy shown in Table 2. This is also the reason why W_{ad} for Al-Al_3Zr models is higher than that of Al-Al_3Sc models in interface 1 modes. Fourthly, in interface 2 modes, the W_{ad} values of Al-Al_3(Zr, Sc) interfaces with Sc elements located at the surface of Al_3(Zr, Sc) phase are higher than others, which is due to the better wetting effect of Sc element. Taking Al-$Al_{24}Zr_7Sc_1$ interface as an example, the interface model with Sc in surface 3 shows a higher W_{ad} value than other three models. And the same results can be seen in other Al_3(Zr, Sc) interface models with different Sc/Zr ratios. This is also the reason why the W_{ad} values of Al-Al_3Sc models are higher than those of Al-Al_3Zr models. Fifthly, the Al-Al_3(Zr, Sc) interfaces formed with two adjacent Sc/Zr layers by central-stacking have higher W_{ad} values than those interfaces formed with two adjacent Sc/Zr layers by top-stacking. This conclusion can be got by comparing the W_{ad} values of Al-$Al_{24}Zr_7Sc_1$, Al- $Al_{12}Zr_3Sc_1$, Al-$Al_6Zr_1Sc_1$, and Al-$Al_{12}Zr_1Sc_3$ interfaces formed with surfaces 1 or 3 to the corresponding interfaces formed with surfaces 2 or 4. All the W_{ad} values of interfaces formed with surface 1 are higher than those of interfaces formed with surface 2. This is also one reason for Al_3(Zr, Sc) refining phase to precipitate in the $D0_{23}$ or $D0_{22}$ structure rather than in the $L1_2$ structure.

In addition, for interface formation, two other factors need to be considered. One is the mismatch of lattice parameter between refining phase and Al matrix. As shown in Table 1, the mismatch of Al_3Sc to Al matrix is only 0.0002 nm, but the mismatch of Al_3Zr to Al matrix is 0.0026 nm. This mismatch will induce lattice distortion energy for interfaces, which hinders the formation of the interface in terms of energy. This is another superiority that Sc atoms are bonded directly with Al matrix instead of Zr atoms. So besides the larger W_{ad} values of the interfaces with Sc atoms located at the surface of refining phase, the simultaneous addition of Sc and Zr elements also reduces the mismatch between Al_3Zr phase and Al matrix. The other one is that lower absolute value of surface energy will result in higher absolute value of interfacial energy, which determines the difficulty level of interface formation. Based on our former investigation[22], Al_3Sc phase has a lower surface energy (1.444 J/m^2) than Al_3Zr phase (1.751 J/m^2), which results in a lower interfacial energy of Al-Al_3Sc interface than Al-Al_3Zr interface. This means that Sc atoms are beneficial to the interface formation and prefer to precipitate along the interfacial sites.

Based on the interfacial properties discussed, the addition of Sc element is beneficial to the formation of the interface, the improvement of the interface bonding strength and wetting effect. But the excessive Sc/Zr ratio shows no good for the improvement of the interface performance. The Sc/Zr ratio controlled no more than 1/3 are beneficial to the improvement of interface performance.

2.4 Partial density of states

In order to understand the interatomic interactions and bonding in the Al_3(Zr, Sc) phase formed under different Sc/Zr ratios, the partial density of states for different Al_3(Zr, Sc) is calculated, as shown in Fig.5. The dashed lines in the figures represent the Fermi level. On the whole, there are a large number of electrons passing through the Fermi level, which reflects the metallic characteristics of the Al_3(Zr, Sc) phases, and the interaction between atoms is dominated by metal bonds. The partial density of states of all Al_3(Zr, Sc) phases exhibits a common feature. The state density distribution of Al-p orbital electrons, Zr-d orbital electrons and Sc-d orbital electrons is very similar, indicating that there are hybrid covalent effects of Al-p orbital electrons, Zr-d orbital electrons and Sc-d orbital electrons. This also explains that in Al_3(Zr, Sc), not only a metal binding but also a covalent interaction between Al-Zr, Al-Sc and Zr-Sc atoms are exhibited. This is the essential reason why the Al_3(Zr, Sc) phase has a large absolute value of binding energy. But for pure Al_3Sc without Zr addition, as shown in Fig.5b, the hybridization of Al-p orbital electrons and Sc-d orbital electrons is weaker than the hybrid covalent effect of Al-p orbital electrons and Zr-d orbital electrons, as shown in Fig.5a, which is clearly shown in the valence band, in the energy range of –4~0 eV. This is also the intrinsic reason for the high binding energy in Al_3Zr.

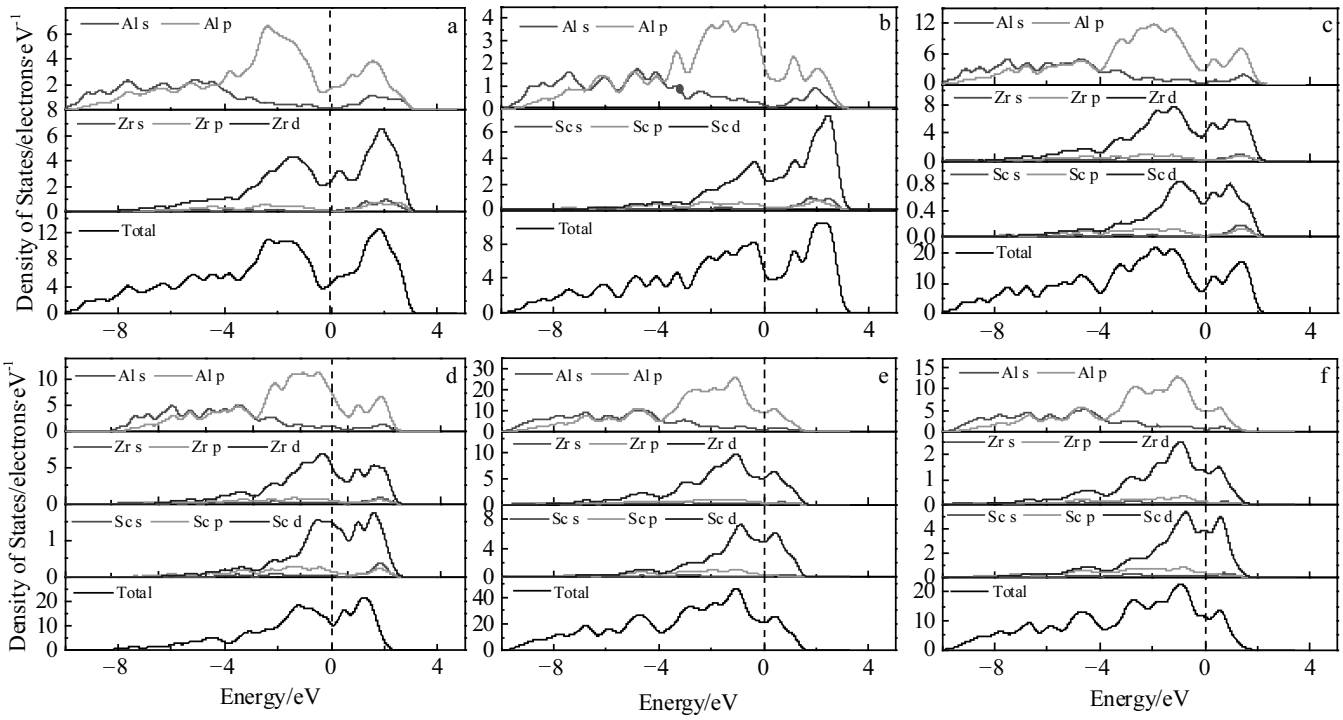

Fig.5 Partial density of states of Al_3(Zr, Sc) with different ratios: (a) Al_3Zr, (b) Al_3Sc, (c) $Al_{24}Zr_7Sc$, (d) $Al_{12}Zr_3Sc$, (e) Al_6ZrSc, and (f) $Al_{12}ZrSc_3$

It can be concluded that the simultaneous addition of Zr and Sc is beneficial to the binding characteristic of the refining phase.

2.5 Electron density difference and bond population

The electron density difference is the difference between the redistributed electron and the electron density of the original isolated atom after the electrons are redistributed by the chemical bond system. Fig.6 shows the electron density difference in (110) crystal planes of Al_3Zr, Al_6ZrSc and Al_3Sc phases, and (100) crystal planes of $Al_{24}Zr_7Sc$, $Al_{12}Zr_3Sc$ and $Al_{12}ZrSc_3$ phases, to keep the facets parallel to the {110} crystal plane of original Al_3Zr phase. Mulliken bond population and atomic charges for Al_3(Zr, Sc) phases with different Sc/Zr ratios are shown in Table 5. Comparing Fig.6a with Fig.6b, the charge transfer between Al and Zr atoms is more obvious than that between Al and Sc atoms, and there are more shared electrons between atoms, indicating that the Al and Zr atoms exhibit stronger covalent interactions. This is consistent with the bond population shown in Table 5. Mulliken bond population for Al-Zr bond around 0.31 is always larger than that of Al-Sc bond around 0.25, which represents the stronger covalent binding between Al and Zr atoms. Table 5 also shows that the atomic charge transfer between Al and Sc atoms is larger than that between Al and Zr

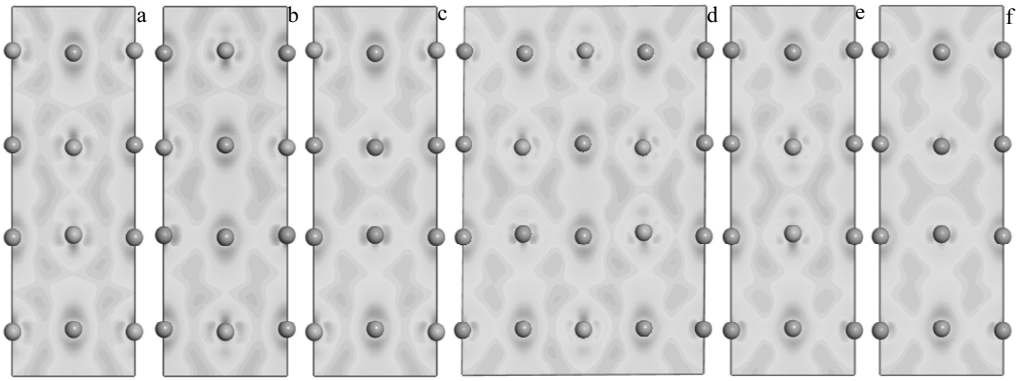

Fig.6 Electron density difference for Al_3(Zr,Sc) phases with different Sc/Zr ratios: (a) Al_3Zr (110), (b) $Al_{24}Zr_7Sc$ (100), (c) $Al_{12}Zr_3Sc$ (100), (d) Al_6ZrSc (110), (e) $Al_{12}ZrSc_3$ (100), and (f) Al_3Sc (110)

Table 5 Mulliken bond population and atomic charges for $Al_3(Zr, Sc)$ phases with different Sc/Zr ratios

Phase	Atom	Charge/e	Bond	Bond population
Al_3Zr	Zr	0.01	Al-Zr	0.31
$Al_{24}Zr_7Sc$	Zr	0.02	Al-Zr	0.31
	Sc	0.28	Al-Sc	0.25
$Al_{12}Zr_3Sc$	Zr	0.02	Al-Zr	0.32
	Sc	0.27	Al-Sc	0.25
Al_6ZrSc	Zr	0.00	Al-Zr	0.34
	Sc	0.27	Al-Sc	0.26
$Al_{12}ZrSc_3$	Zr	0.00	Al-Zr	0.32
	Sc	0.26	Al-Sc	0.27
Al_3Sc	Sc	0.24	Al-Sc	0.26

atoms. Between Al and Zr atoms, there is almost no net charge transfer. And this phenomenon is also verified by electron density difference shown in red parts in Fig.6. All these are consistent with the density of states shown in Fig.5 and result in the larger binding energy of Al_3Zr compared to Al_3Sc phase.

3 Conclusions

1) The calculation results show that the formation energy of the $Al_3(Zr, Sc)$ with simultaneous addition of Zr and Sc is larger than that of Al_3Sc phase formed by the single addition of Sc. This means that the larger nucleation driving force of $Al_3(Zr, Sc)$ is beneficial to the refinement phase. Dispersion and precipitation can effectively improve the effect of refining crystal grains while greatly reduce costs. Besides, $Al_3(Zr, Sc)$ formed with simultaneous addition of Zr and Sc has a larger absolute value of the binding energy than the Al_3Sc phase, indicating that the $Al_3(Zr, Sc)$ phase is more difficult to decompose, and can act better as a pinning phase to inhibit recrystallization during heat treatment or deformation. Further, when the Sc/Zr ratio is lower than 1/3, the binding energy of $Al_3(Zr, Sc)$ microalloying phase and their absolute value of the formation enthalpy are larger than those of the phases with Sc/Zr ratio higher than 1/3. It is shown that when the Sc/Zr ratio is lower than 1/3, the $Al_3(Zr, Sc)$ microalloying phase is more likely to precipitate and has better stability.

2) Elastic property studies show that the simultaneous addition of Zr and Sc can effectively improve the elastic properties of Al_3Sc. The $Al_3(Zr, Sc)$ microalloying phases with Sc/Zr ratio lower than 1/3 have better elastic properties than those with Sc/Zr ratio higher than 1/3. Among them, when Sc/Zr ratio is equal to 1/7, the elasticity and plasticity of $Al_3(Zr, Sc)$ phase are the best. Under the condition that Sc/Zr ratio is equal to 1/3, the rigidity of $Al_3(Zr, Sc)$ phase is the strongest and anisotropy is the weakest. In the $Al_3(Zr, Sc)$ microalloying phase, the metal binding dominates between the atoms and strong covalent interaction exists, which determines the large binding energy and high melting point of the $Al_3(Zr, Sc)$ microalloying phase and is the intrinsic reason why it is suitable to act as refining phases in aluminum alloys.

3) Interfacial properties of $Al_3(Zr, Sc)$ and Al matrix show that the addition of Sc element is beneficial to the formation of the interface, the improvement of the interface bonding strength and interfacial wetting effect. But the excessive Sc/Zr ratio shows no positive effect on the improvement of the interface performance. The Sc/Zr ratio controlled no more than 1/3 is beneficial to the improvement of interface performance. Combing the nucleation and elastic properties of $Al_3(Zr, Sc)$ phases with their interfacial properties, it can be concluded that the preferred Sc/Zr ratio in experiments should be 1:3.

References

1 Xu Xuesong, Zheng Jingxu, Li Zhi *et al*. *Materials Science and Engineering A*[J], 2017, 691: 60

2 Marlaud T, Deschamps A, Bley F *et al*. *Acta Materialia*[J], 2010, 58(1): 248

3 Li C M, Zeng S M, Chen Z Q *et al*. *Computational Materials Science*[J], 2014, 93: 210

4 Dinaharan I, Ashok Kumar G, Vijay S J *et al*. *Materials & Design*[J], 2014, 63: 213

5 Deng Ying, Xu Guofu, Yin Zhimin *et al*. *Journal of Alloys and Compounds*[J], 2013, 580: 412

6 Srinivasan S, Desch P B, Schwarz R B. *Scripta Metallurgica et Materialia*[J], 1991, 25(11): 2531

7 Mikhaylovskaya A V, Mochugovskiy A G, Levchenko V S *et al*. *Materials Characterization*[J], 2018, 139: 30

8 Huang Hanqing, Wang Weicheng, Yuan Qiuhong *et al*. *Philosophical Magazine*[J], 2019, 99(8): 971

9 Wang R N, Tang B Y, Peng L M *et al*. *Computational Materials Science*[J], 2012, 59: 87

10 Knipling K E, Karnesky R A, Lee C P *et al*. *Acta Materialia*[J], 2010, 58(15): 5184

11 Forbord B, Lefebvre W, Danoix F *et al*. *Scripta Materialia*[J], 2004, 51(4): 333

12 Duan Y L, Xu G F, Peng X Y *et al*. *Materials Science and Engineering A*[J], 2015, 648: 80

13 Knipling K E, Seidman D N, Dunand D C. *Acta Materialia*[J], 2011, 59(3): 943

14 Li B, Pan Q, Huang X *et al*. *Materials Science and Engineering: A*[J], 2014, 616: 219

15 Lohar A K, Mondal B, Rafaja D *et al*. *Materials Characterization*[J], 2009, 60(11): 1387

16 Sun Fangfang, Nash G L, Li Qunying *et al*. *Journal of Materials Science & Technology*[J], 2017, 33(9): 1015

17 Ikeshita S, Strodahs A, Saghi Z *et al*. *Micron*[J], 2016, 82: 1

18 Li J H, Wiessner M, Albu M *et al*. *Materials Characterization*[J], 2015, 102: 62

19 Vlach M, Čížek J, Smola B *et al*. *Materials Characterization*[J], 2017, 129: 1

20 Vlach M, Stulikova I, Smola B *et al*. *Materials Characterization* [J], 2013, 86: 59

21 Yu Kun, Li Wenxian, Li Songrui *et al*. *Materials Science and Engineering A*[J], 2004, 368(1-2): 88

22 Li Chunmei, Cheng Nanpu, Chen Zhiqian *et al*. *Materials*[J], 2018, 11(4): 636
23 Vanderbilt D. *Physical Review B*[J], 1990, 41(11): 7892
24 Segall M D, Lindan P J D, Probert M J *et al*. *Journal of Physics: Condensed Matter*[J], 2002, 14(11): 2717
25 Perdew J P, Chevary J A, Vosko S H *et al*. *Physical Review B*[J], 1992, 46(11): 6671
26 Perdew J P, Burke K, Ernzerhof M. *Physical Review Letters*[J], 1996, 77(18): 3865
27 Monkhorst H J, Pack J D. *Physical Review B*[J], 1976, 13(12): 5188
28 Milman V, Warren M C. *Journal of Physics: Condensed Matter* [J], 2001, 13: 241
29 Zhao J J, Winey J M, Gupta Y M. *Physical Review B*[J], 2007, 75(9): 94 105
30 Deyirmenjian V B, Heine V, Payne M C *et al*. *Physical Review B*[J], 1995, 52(21): 15 191
31 Wang S Q, Ye H Q. *Journal of Physics: Condensed Matter*[J], 2003, 15: 5307
32 Li J, Zhang M, Zhou Y *et al*. *Applied Surface Science*[J], 2014, 307: 593
33 Ghosh G, Asta M. *Acta Materialia*[J], 2005, 53(11): 3225
34 Amador C, Hoyt J J, de Fontaine D *et al*. *Physical Review Letter*[J], 1995, 74(24): 4955
35 Colinet C, Pasturel A. *Journal of Alloys and Compounds*[J], 2001, 319: 154
36 Kematick R J,Franzen H F. *Journal of Solid State Chemistry*[J], 1984, 54: 226
37 Ghosh G, Vaynman S, Asta M *et al*. *Intermetallics*[J], 2007, 15(1): 44
38 Huang Yuanchun, Guo Xiaofang, Ma Yunlong *et al*. *Physica B: Condensed Matter*[J], 2018, 548: 27
39 Hu Wencheng, Liu Yong, Li Diangli *et al*. *Physica B: Condensed Matter*[J], 2013, 427: 85
40 Deng Ying, Yin Zhimin, Pan Qinlin *et al*. *Journal of Alloys and Compounds*[J], 2017, 695: 142
41 Hu Hai, Zhao Mingqi, Wu Xiaozhi *et al*. *Journal of Alloys and Compounds*[J], 2016, 681: 96

铝合金细化相 $Al_3(Zr, Sc)$的能量、弹性与界面性质的第一性原理研究

李春梅，蒋显全，程南璞，唐剑锋，陈志谦
(西南大学，重庆 400715)

摘　要：微合金化是强化铝合金的重要手段，Sc 作为铝合金有效的细化剂而引起广泛关注。在铝基体中同时添加 Zr 和 Sc 将在铝基体中形成 $Al_3(Zr, Sc)$细化相可以实现更好的晶粒细化。基于密度泛函理论的第一性原理方法，研究了不同 Sc/Zr 配比下形成的 $Al_3(Zr, Sc)$细化相的能量和弹性性质。结果表明，当 Sc/Zr 比不大于 1/3 时，$Al_3(Zr, Sc)$相具有较大的形成焓绝对值，细化相将优先于 $Al_3(Zr, Sc)$相析出。同时，Sc 元素的加入有利于界面的形成，提高界面的结合强度和润湿效果，但大于 1/3 的 Sc/Zr 比对界面性能的提高并无积极作用。并且，Zr 的加入可以有效提高细化相的弹性性能，并削弱 Al_3Sc 的弹性各向异性特征。此理论研究指出，微合金化 Zr 和 Sc 的共同添加且 Sc/Zr 比不大于 1/3 时，可以保证细化效果并大大降低合金的成本。

关键词：细化相；形成焓；弹性性质；界面性能；$Al_3(Zr, Sc)$

作者简介：李春梅，女，1980 年生，博士，副教授，西南大学材料与能源学院，重庆 400715，电话：023-68254376，E-mail: lcm1998@swu.edu.cn